Minor bodies in the outer Solar System

Planets and Astrobiology (2020-2021)

G. Vladilo and S. Ivanovski

Transneptunian objects (Kuiper belt)

- The discovery of Pluto in 1930 suggested that a debris disk of icy material could be present in the outer Solar System

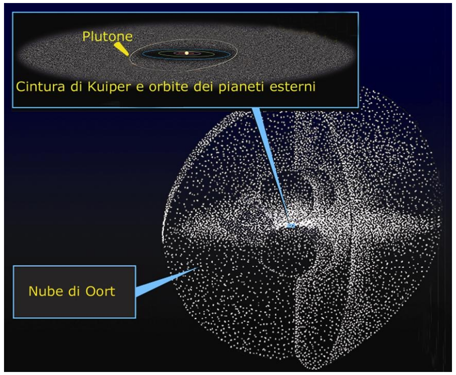

- The existence of such disk was predicted independently by Edgeworth and Kuiper ~1940-1950
  - Hypothesis: the disk of small bodies that formed the giant planets perhaps extended past Neptune, with a density too low (or perhaps the formation times too long) to form planets; small bodies that did not succeed to form a planet should still be there
  - Transneptunian objects were to faint to be observed with telescopes of that time
  - Dynamical studies showed that the mass of the debris disk should be no more than 1.3 Earth masses

Transneptunian objects (Kuiper belt)

- Around 1980 it was proposed that the hypothetical disk of small bodies beyond Neptune (called the “Kuiper Belt”) could be the source reservoir for short-period comets
  - This proposal led observers to search for small bodies in the Kuiper belt with the astronomical instrumentation of new generation
  - The first detection of a Kuiper belt object came in 1992
  - Currently we know about a thousand KBOs
  - We estimate that $\sim 10^5$ KBOs with diameter > 50 km may exist

1992 QB1

Discovery of the first trans-Neptunian object

TNOs are hard to observe:

Flux vary with p x D^2 x R^{-4}

An object with given size D and albedo p is 10^4 times fainter beyond Neptune (R = 30 au) than in the asteroid belt (R = 3 au)

distance 41.2 AU

magnitude 23.5

10^7 fainter than a star at naked eye

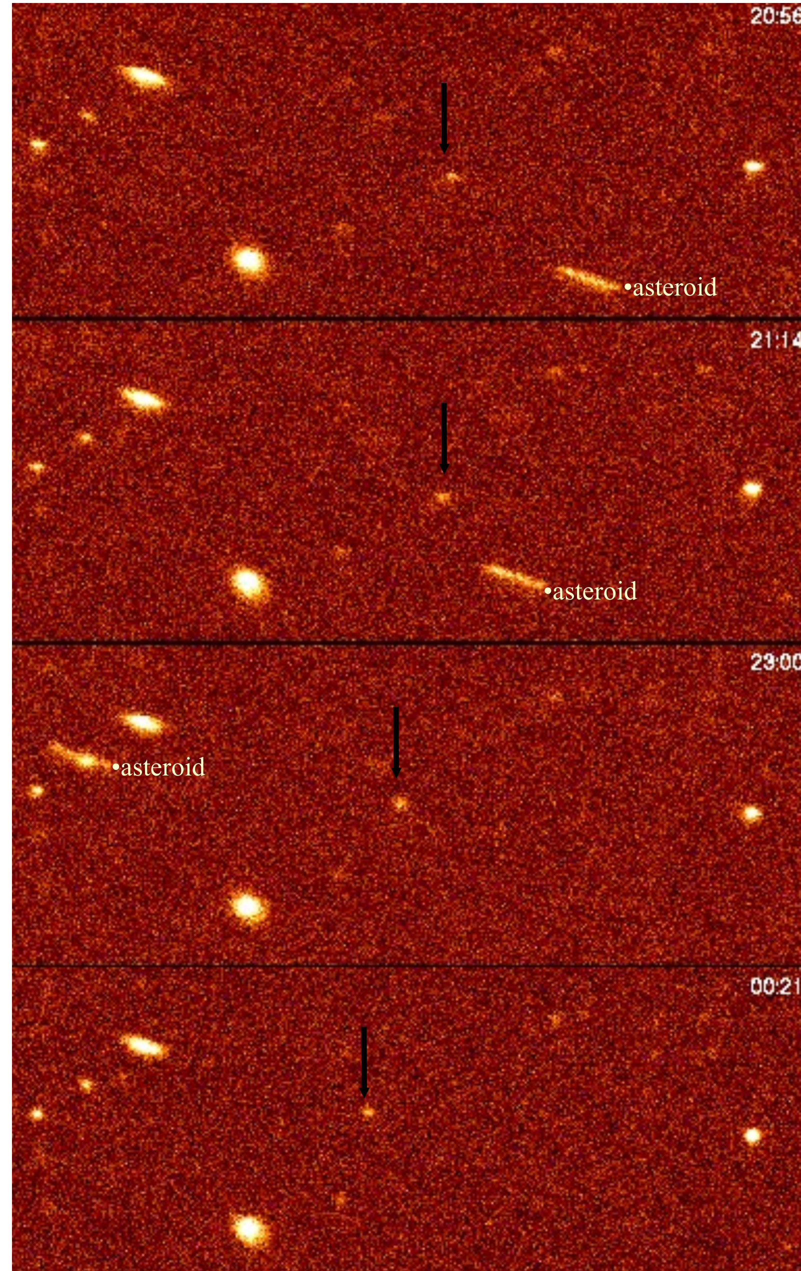

Detection of minor objects of the outer Solar System from measurements of proper motion

- Motion of a Solar System object relative to the background stars and galaxies
  - Comparison of two 300 sec images taken with the 10-m Keck telescope at an interval of one hour. A body with high proper motion relative to the fixed background pattern is found. The proper motion is due to the Earth's and the body's revolution about the Sun. Such motion is how we discover minor bodies of the outer Solar System.

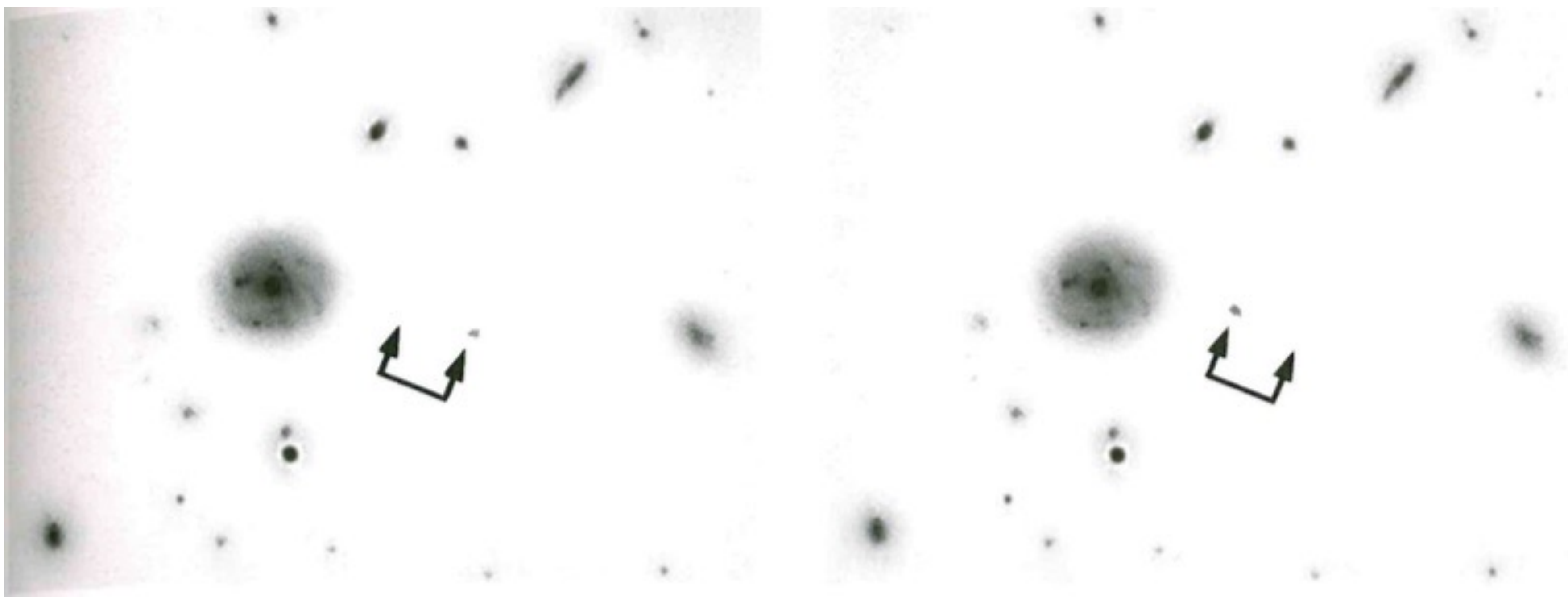

Dynamical classification of transneptunian objects

Distribution of KBOs with well determined orbits
Top panels: inclinations. Bottom panels: eccentricities.
Blue dots: *classical Kuiper Belt*. Red dots: *scattered disk*.
Green dots: *resonant populations*.
Vertical lines: 3:4, 2:3, 1:2 mean motion resonances with Neptune.
Big crossed circle: Pluto. Dotted curves: perihelion distances 30 and 35 AU

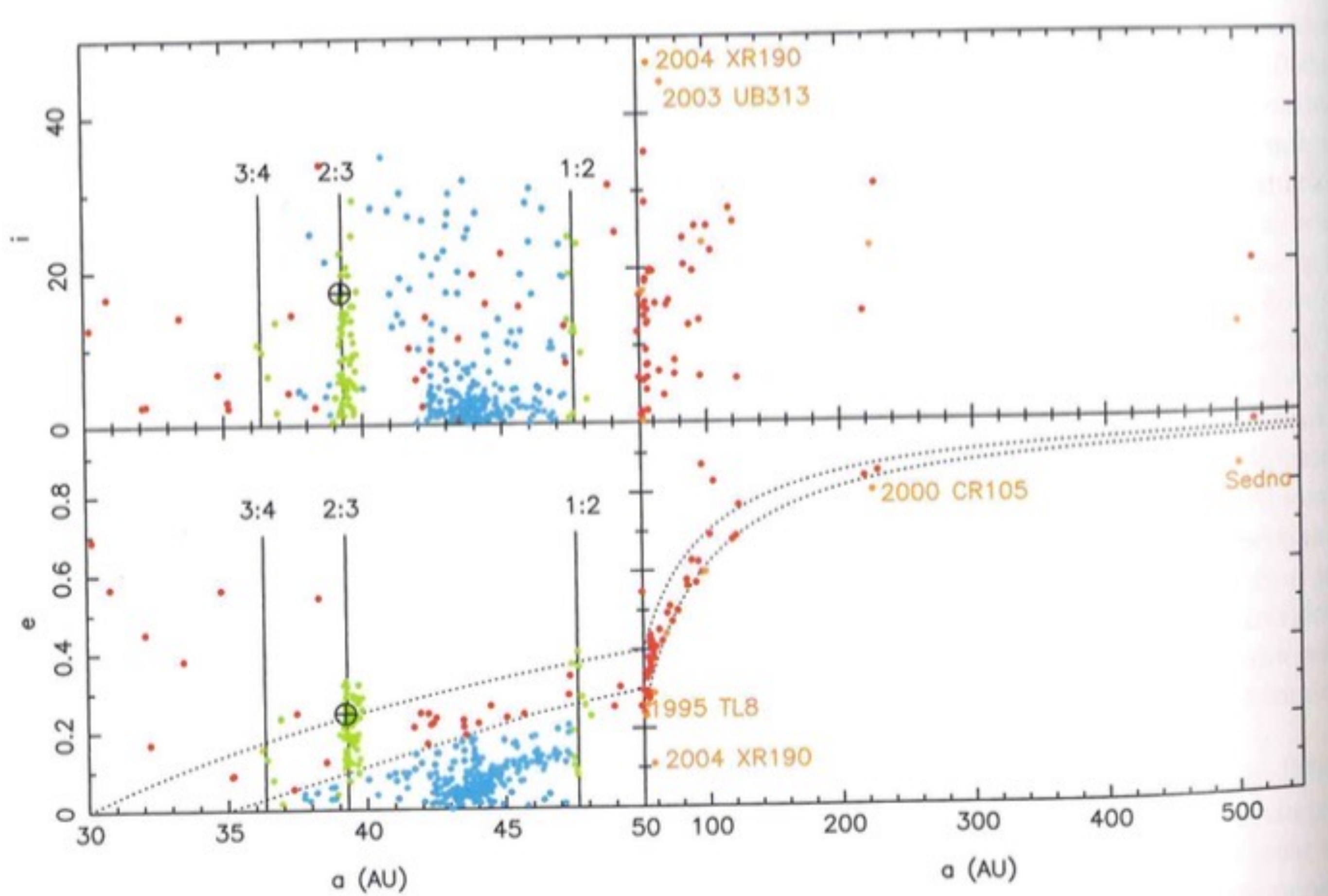

Centaur objects

- Centaur objects are recent escapees from the Kuiper Belt
  - They are on elliptical orbits about the Sun that cross the near-circular orbits of Saturn, Uranus and Neptun
  - Within a few tens of millon years after a Centaur object escapes from the Kuiper Belt, the giant planets scatter it into the Sun or a planet, or cause it to migrate into the region of terrestrial planets
  - By virtue of their relatively close approach, many Centaur objects become bright enough for certain physical studies that are not possible on fainter KBOs

Recent census of minor bodies in the outer Solar System

Red dots: KBOs

THE OUTER SOLAR SYSTEM

This animation shows the motion of the outer part of the solar system over a 100-year time period. The sun is at the center and the orbits of the planets Jupiter, Saturn Uranus and Neptune are shown in light blue (the locations of each planet are shown as large crossed circles).

Comets: blue squares (filled for numbered periodic comets, outline for other comets)
High-e objects: cyan triangles
Centaurs: orange triangles
Plutinos: white circles (Pluto itself is the large white crossed circle)
"Classical" TNOs: red circles
Scattered Disk Objects: magenta circles

The individual frames were generated on an OpenVMS system, using the PGPLOT graphics library. The animation was put together on a RISC OS 4.03 system using !InterGif.

Orange triangles: Centaurs

http://www.minorplanetcenter.net

Recent census of minor bodies in the outer Solar System

Red dots: KBOs

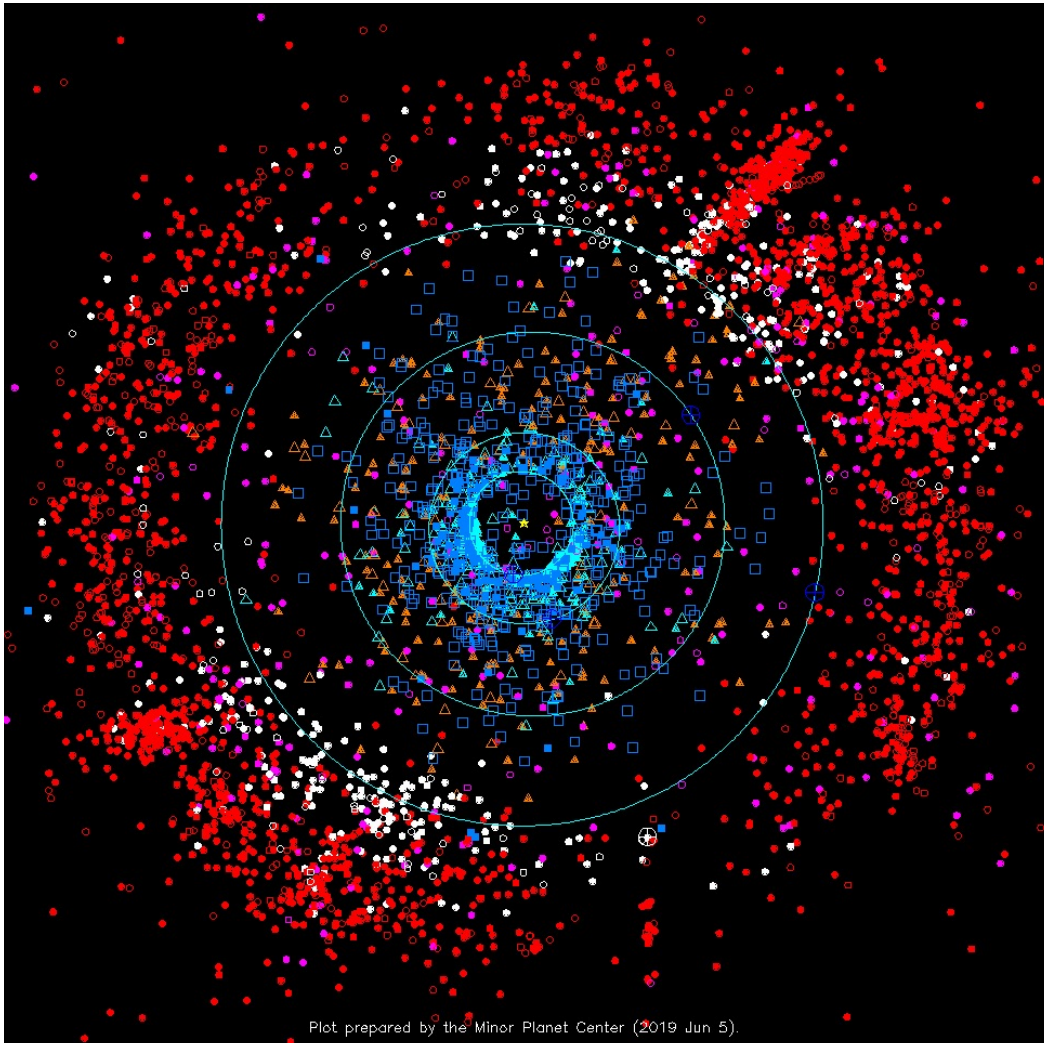

Orange triangles: Centaurs

http://www.minorplanetcenter.net

Trans-Neptunian Objects and Centaurs

Gladman et al. (2008)

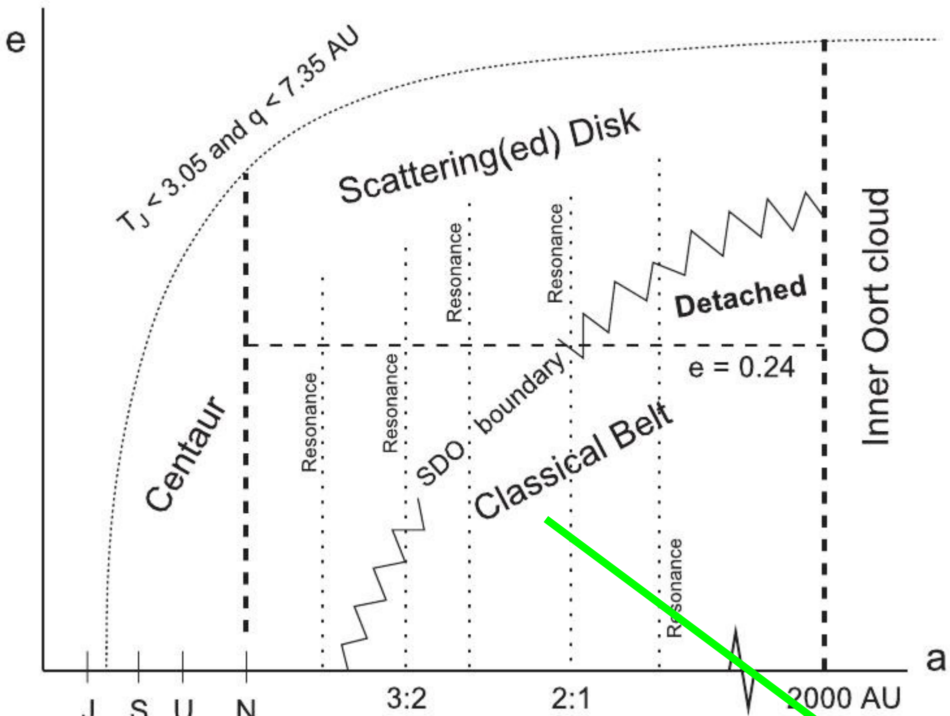

$$T_P = \frac{a_P}{a} + 2 \cdot \sqrt{\frac{a}{a_P}(1-e^2)} \cos i$$

Tisserand's parameter

q - perihelion

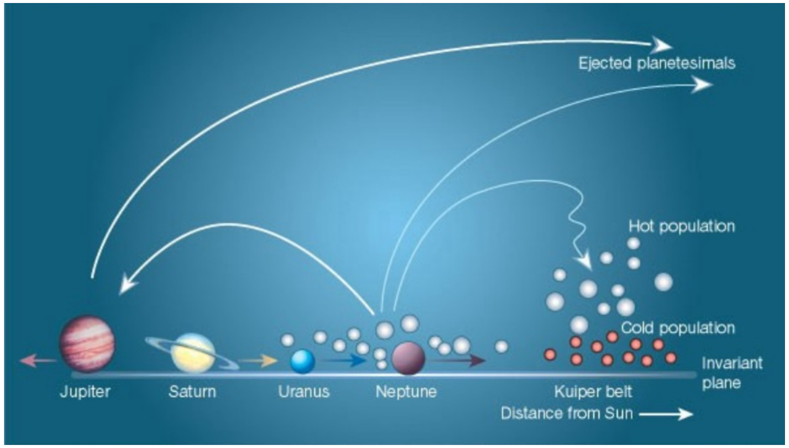

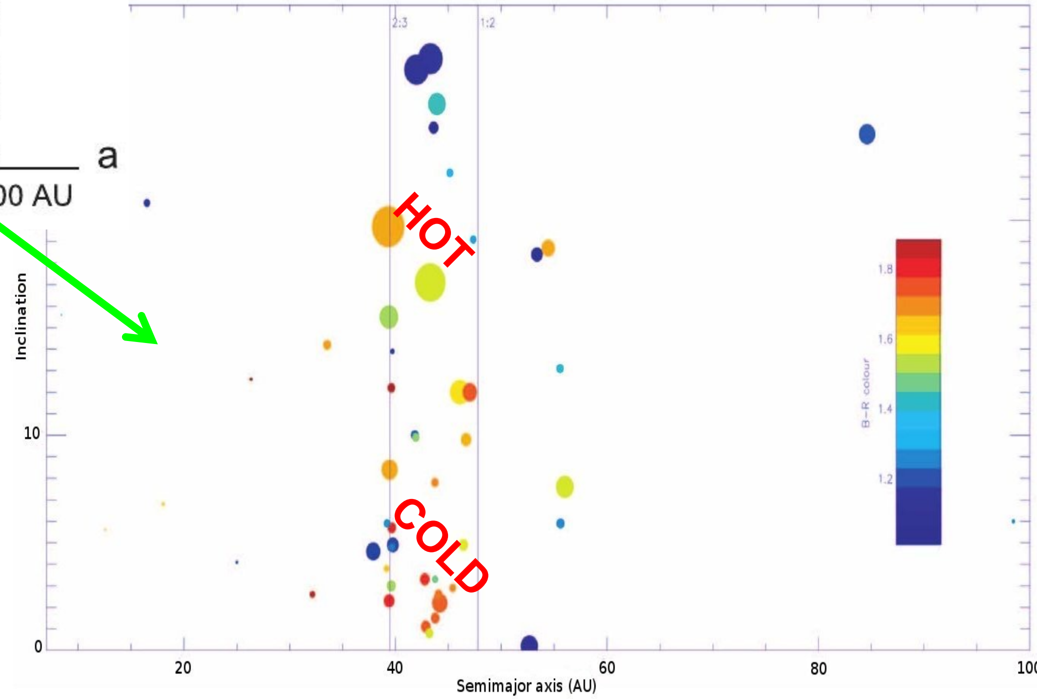

Characterization of Kuiper Belt and Centaur objects

- Rotation of KBOs
  - Left: rotation of a non-spherical KBO or Centaur object results in a periodic variation of the object's projected area on the plane (top) of the sky and hence a periodic variation in its brightness (bottom), i.e. a *lightcurve*
  - Right: lightcurve for the Centaur Pholus

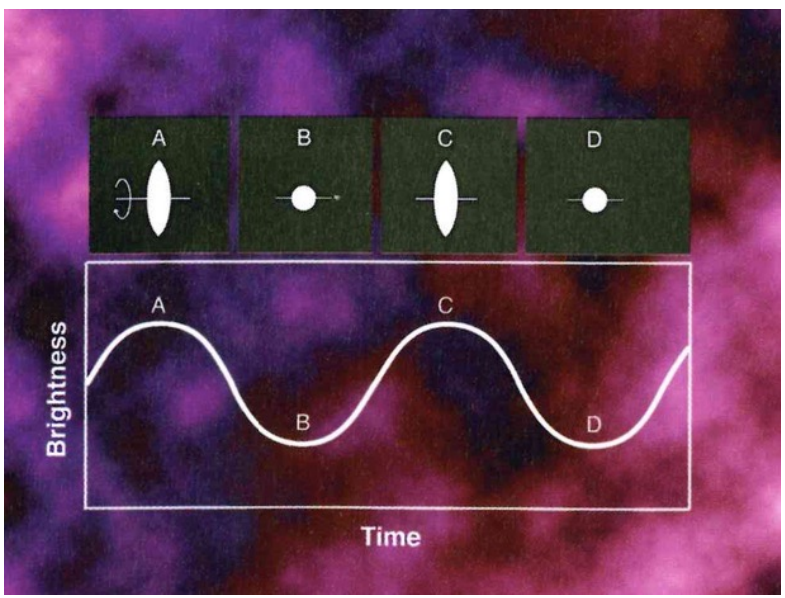

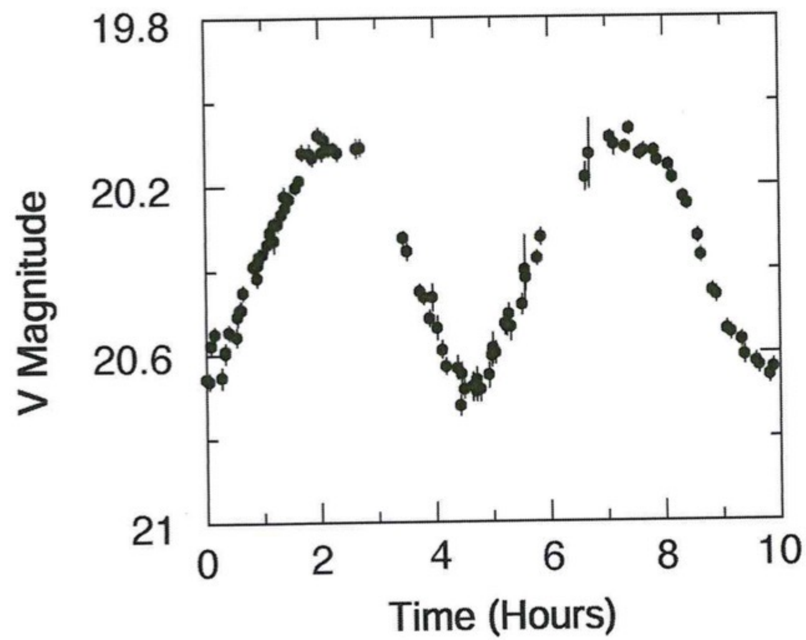

Characterization of Kuiper Belt objects

- Near infrared spectra of KBOs
  - The spectra of Pluto exhibits strong CH_4 ice bands
  - The spectra of Charon (Pluto's satellite) and Quaoar (a classical belt KBO) exhibit strong H_2O absorption bands at 1.5, 1.65 and 2.0 µm

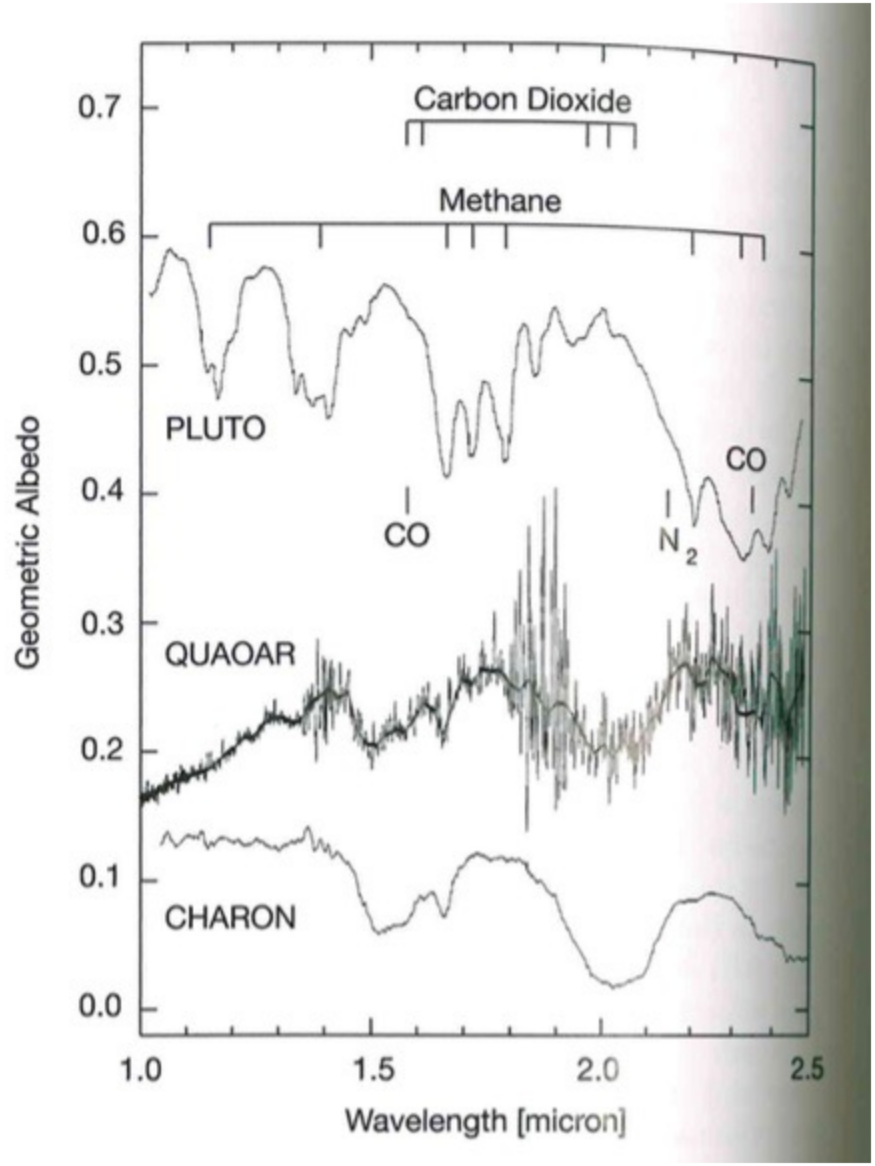

Transneptunian dwarf planets

Name	region	M [M_{Moon}]	ρ [g/cm^3]	a [AU]	e	i [º]
Ceres	Asteroid belt	0.013	2.1	2.77	0.078	10.6
Pluto	Kuiper belt	0.178	2.0	39.5	0.249	17.1
Eris	Scattered disk	0.227	2.5	67.7	0.442	44.2

The difference in orbital properties suggest different origins

Orbits tend to be eccentric and tilted

Masses are small, even compared to Moon's mass

Mean densities are intermediate between the values typical of silicates and ices

Many other dwarf planets probably exist in the Kuiper belt

Pluto

New Horizon observations

Launched: 2006 | Fly-by of Pluto-Charon: 2016 | Fly-by of other TNO: 2017-2023

Evidence for water-ice crust, geologically young surface units, surface ice convection, wind streaks, volatile transport, and glacial flow

Extended atmosphere with trace hydrocarbons and a surface pressure ~10 microbars; a global haze layer

The diverse surface geology and long-term activity raise fundamental questions about how small planets remain active many billions of years after formation

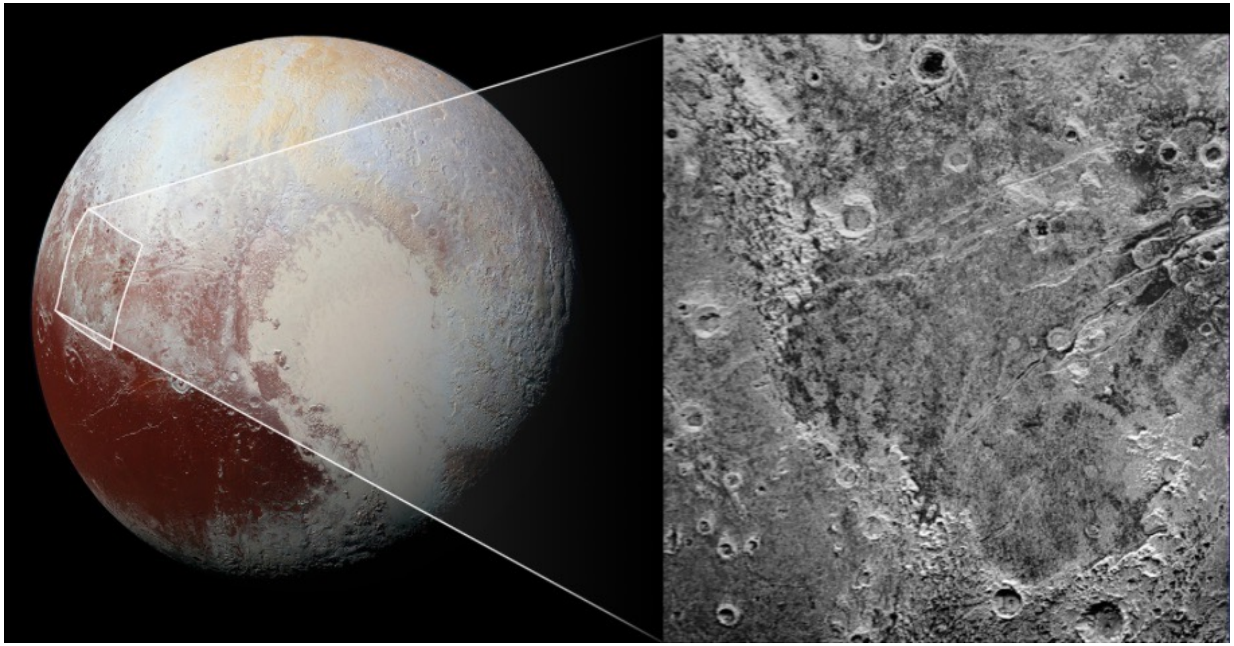

Comets

- Solid debris of the outermost regions of the Solar System
  - Believed to be more pristine (less processed) than asteroids/meteorites
  - Inhomogeneous population

    Formed over a large interval of distances and temperatures

- Here we examine some characteristics:
  - Classification
  - Activity
  - Evolution
  - Chemical composition

Comet classification

- Based on the orbital period
  - Long period comets (LP)

    $P > 200$ yr
  - Short period comets (SP)

    $P < 200$ yr

    If $P > 30$ yr $\Rightarrow$ Halley type

    If $P < 30$ yr $\Rightarrow$ Jupiter type

- Based on their origin in the Solar System
  - For most the time, comets lie within two reservoirs:

    the *Kuiper belt* and the *Oort Cloud*

- Cometary orbits can vary significantly, changing the location of a comet in the Solar System, due to dynamical instabilities driven by gravitational perturbations

The Oort Cloud

- Extended distribution of comets with random inclination of the orbits
  - Cloud with spherical symmetry
  - May comprise billons of comets
- Extends up to 5 x 10^4 AU
  - Up to the limit of gravitational perturbations from nearby stars

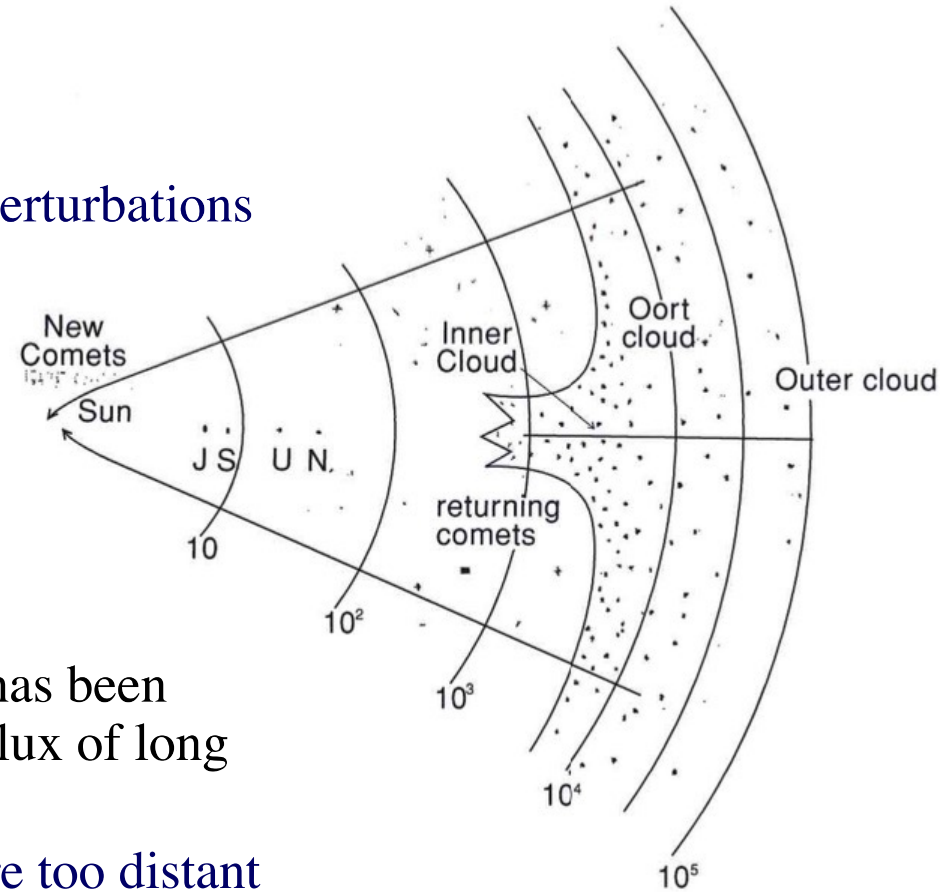

- The existence of the Oort Cloud has been invoked to explain the observed flux of long period comets
  - The comets of the Oort Cloud are too distant and inactive to be observable from Earth

Origin and dynamical evolution of comets

- It is believed that the comets of the Oort Cloud did not originate in situ, but instead they ended up in the Oort Cloud as a result of gravitational scattering in the region of giant planets
- Comets from the Kuiper Belt are instead believed to originate in situ, later becoming Centaurs and finally Jupiter-family comets

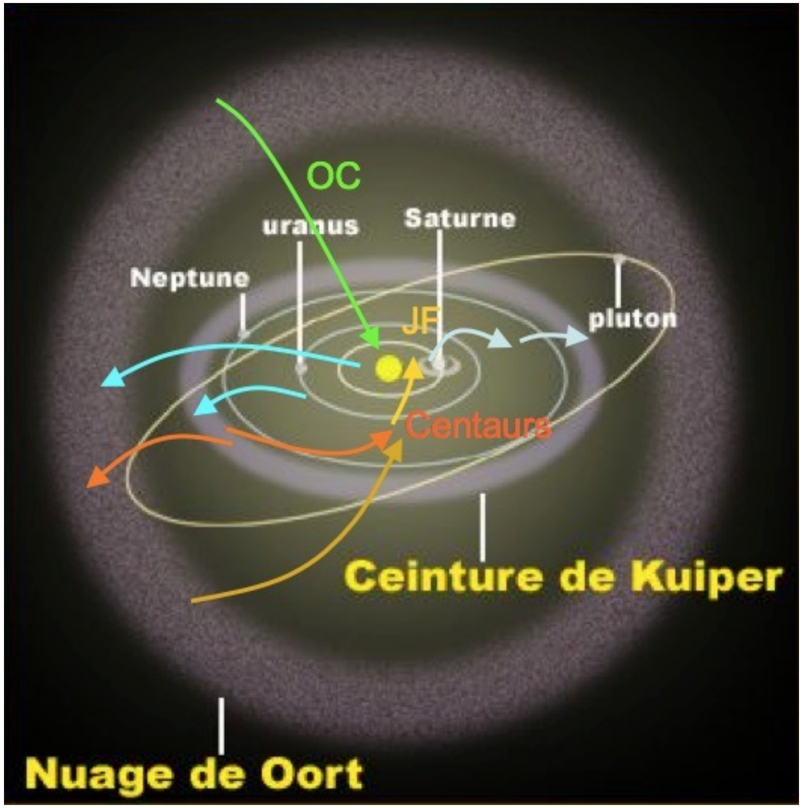

Cometary activity

- If a comet approaches the Sun, the rise of insolation triggers a release of gas, dust and rocks

- The outgoing material generates a rarified atmosphere, called "coma"
  - A spheroidal hydrogen coma, due Lyman alpha radiation, is visible in the ultraviolet spectral range

- The radiation pressure and the solar wind, by interacting with coma, create the characteristic cometary tails
  - Cometary tails can attain sizes larger than 10^6 km
  - Dust and ions form different types of cometary tails

- The dust tail is observable when it reflects the solar light
  - The dust tail is generated by the solar radiation pressure and can bend following the comet's trajectory

- The ejected gas becomes ionized, creating a plasma tail
  - Ionization takes place via:

    (1) <u>photoionization</u> by UV solar radiation

    (2) <u>charge transfer</u> with particles of the solar wind
  - The plasma tail is sweeped by the solar wind and is aligned with the Sun direction

Comet Hale-Bopp
White: dust tail
Blue: plasma tail

Schematic of cometary features and phenomena

[distances on a logarithmic scale]

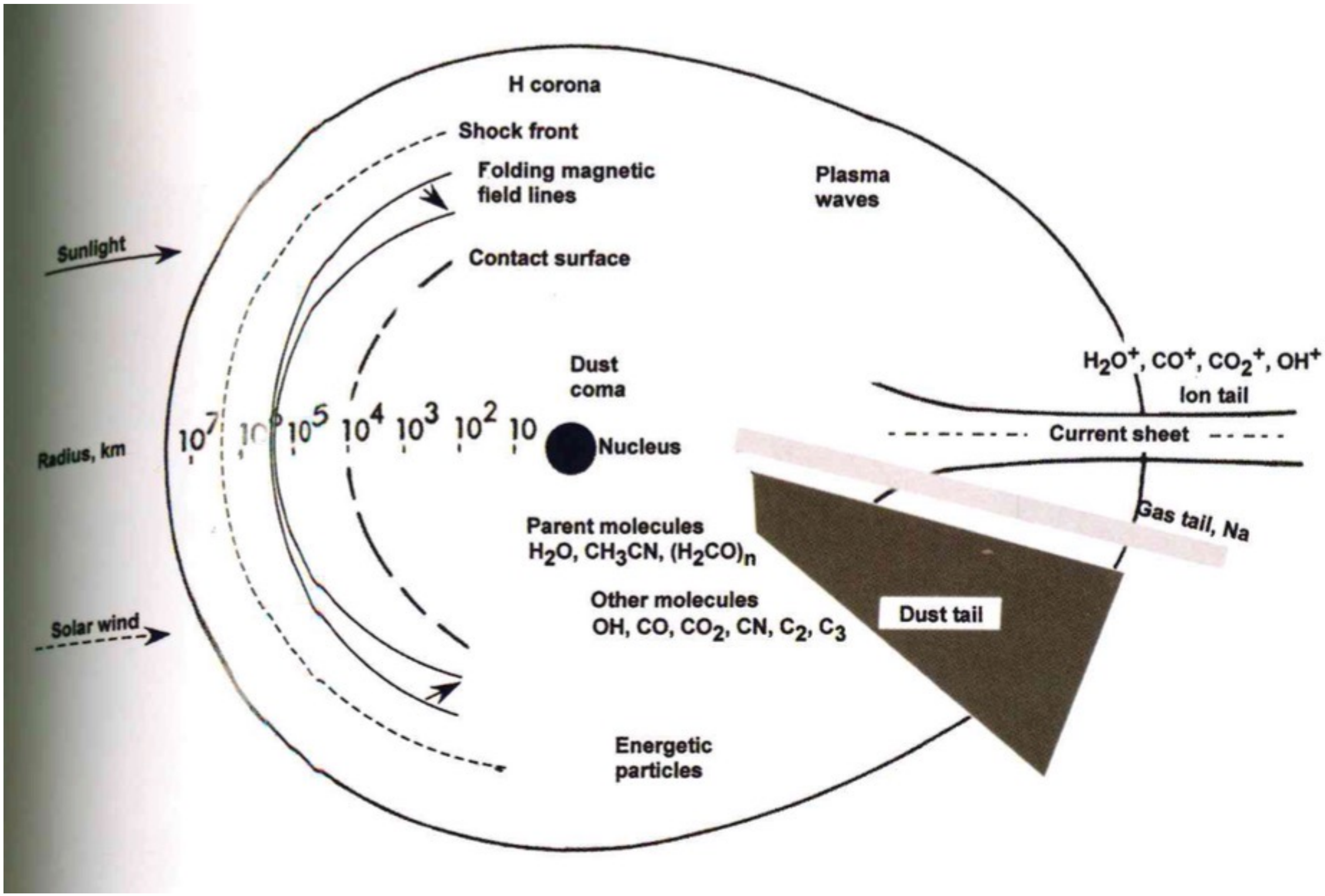

Cometary nucleus

Schematic of the physical processes at work

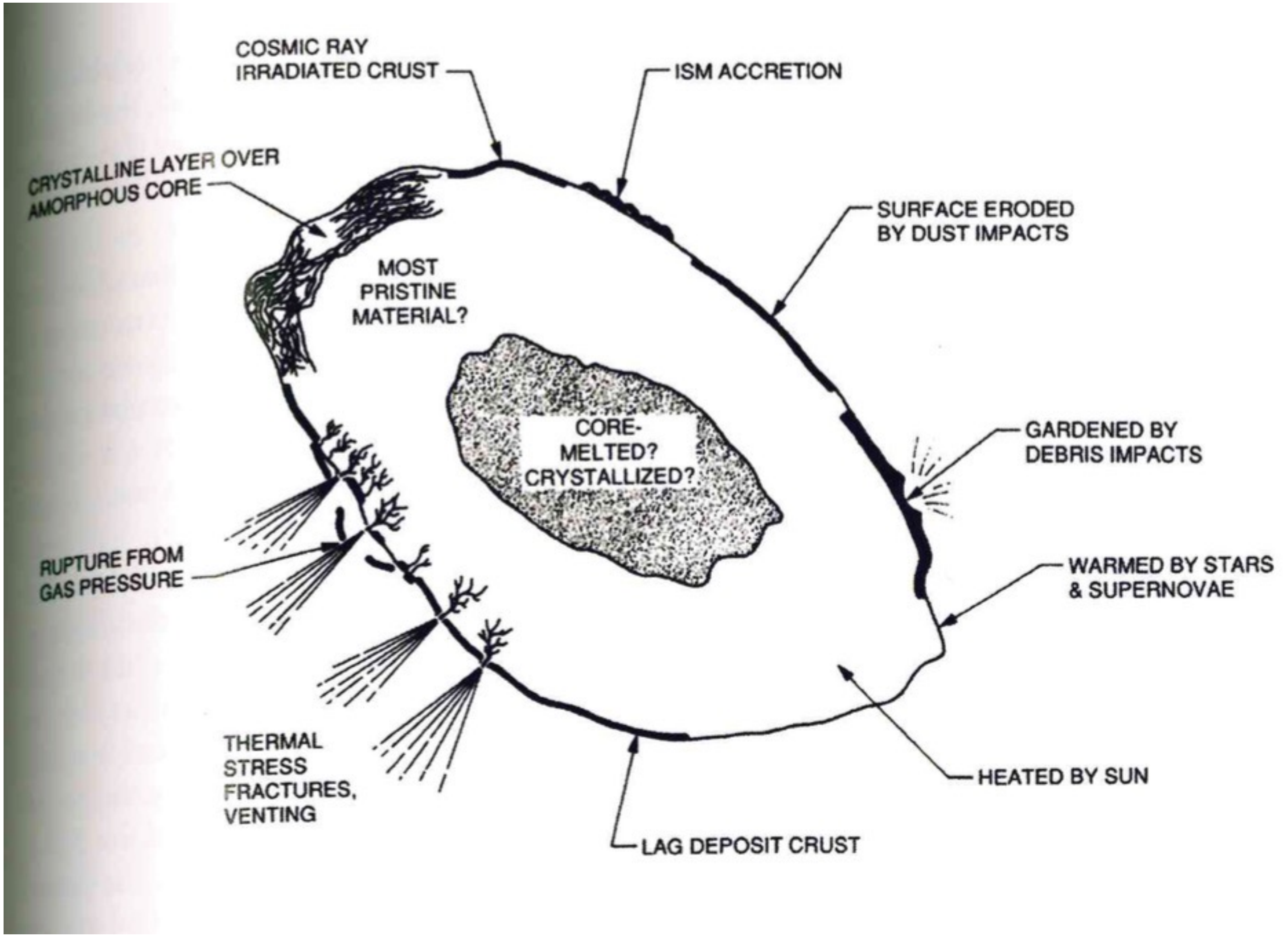

Nucleus of comet P/67 Rosetta mission (ESA)

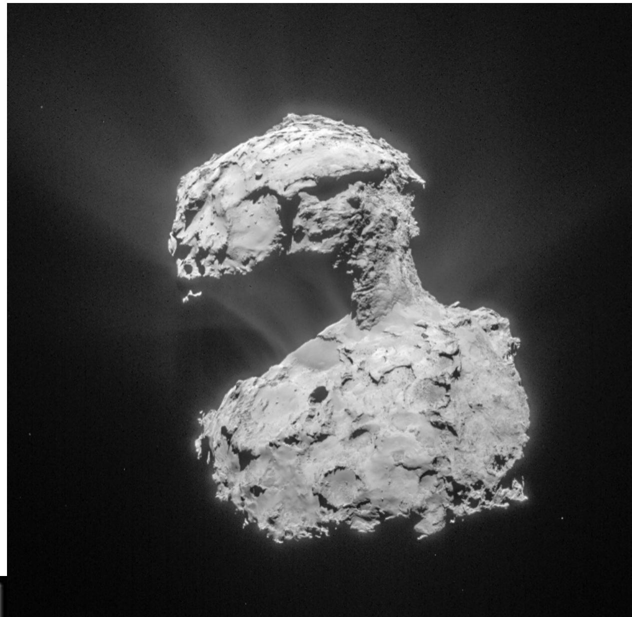

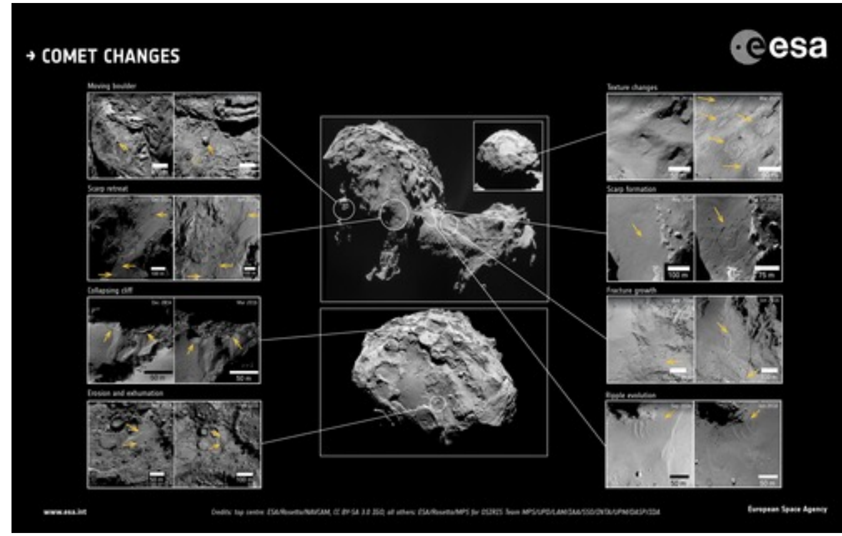

Rotating dust grains in the coma of comet 67P

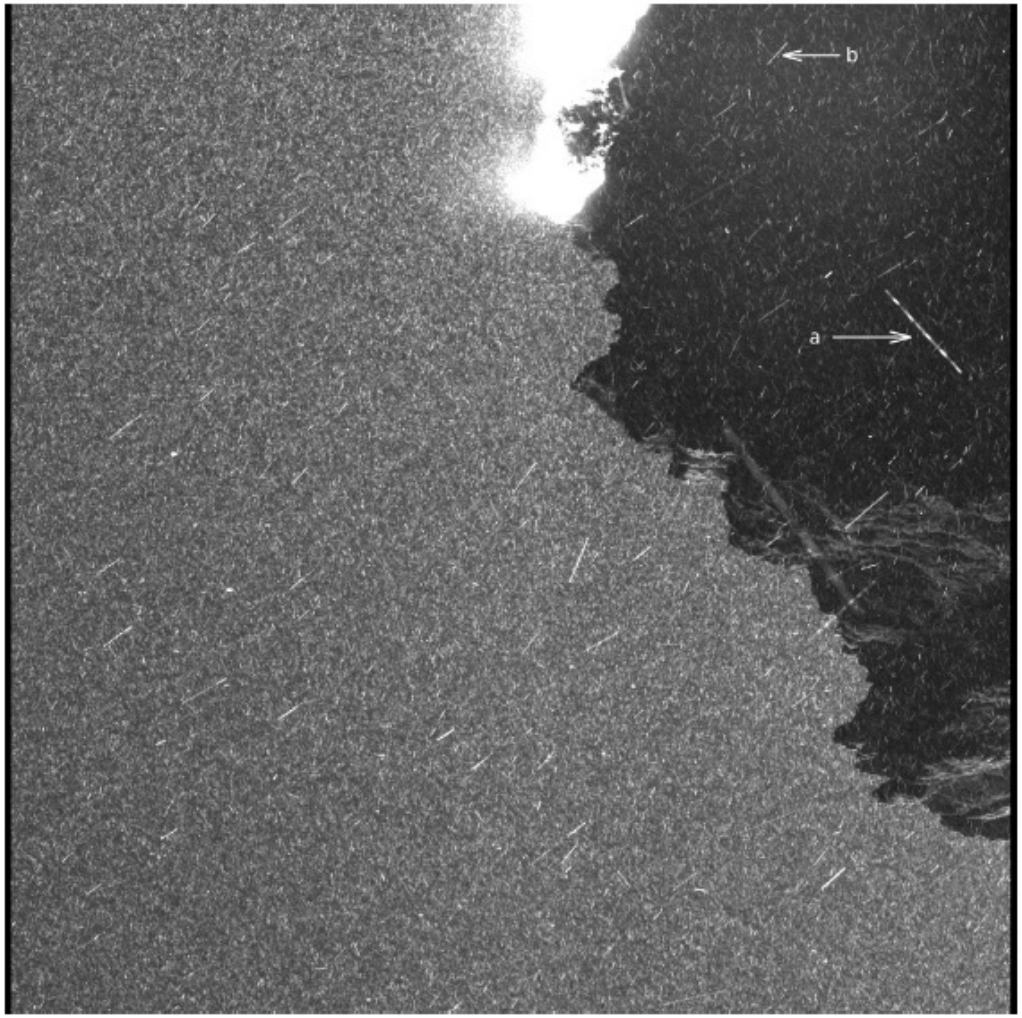

Fig. 1. OSIRIS NAC image taken on 22 October 2014, 01h17m12s UT. The dust coma is resolved in single particles of subpixel apparent sizes, visible as tracks due to proper and spacecraft motion during the exposure time of 5.7 s. Some tracks show a periodic brightness variation during the exposure. The light curves of tracks marked by labels a and b are shown in Fig. 2.

Table 1. Parameters of the simulations are the gas production rate Q_g, the grain bulk density ρ_d and the initial grain orientation α_0.

Case	Q_g [s^{-1}]	b [m]	ρ_d [kg m^{-3}]	α_0 [deg]	L_∞ [m]	t_∞ [s]	v_∞ [m s^{-1}]	ν_∞ [Hz]	L_{90} [m]	t_{90} [s]	t_{rs} [s]	Δ_{max} [Hz]	Δ_{min} [Hz]
#omd1a1	5×10^{26}	10^{-3}	100	22.5	26 211	8000	3.5	0.06	8149	2700	1050	0.11	0.09
#omd2a1	5×10^{26}	10^{-3}	700	22.5	8574	9000	1.0	0.02	6614	7000	3300	0.04	0.03
#omd3a1	5×10^{26}	10^{-3}	1000	22.5	6273	9000	0.7	0.02	4934	7000	4450	0.03	0.03
#pmd1a1	5×10^{26}	10^{-3}	100	22.5	20 277	8000	2.74	–	7602	3200	–	0.02	0.01
#pmd2a1	5×10^{26}	10^{-3}	700	22.5	5713	9000	0.6	–	4272	6600	–	0.008	0.004
#pmd3a1	5×10^{26}	10^{-3}	1000	22.5	3550	9000	0.3	–	3311	8200	–	0.006	0.006
#omd1a2	5×10^{26}	10^{-3}	100	45.0	27 856	8000	3.7	0.03	7775	2400	2100	0.06	0.05
#omd2a2	5×10^{26}	10^{-3}	700	45.0	9519	9000	1.1	0.01	5222	4950	6600	0.03	0.02
#omd3a2	5×10^{26}	10^{-3}	1000	45.0	7152	9000	0.8	0.01	4531	5600	8600	0.03	0.02
#pmd1a2	5×10^{26}	10^{-3}	100	45.0	18 858	8000	2.5	0.01	6746	3000	3200	0.04	0.02
#pmd2a2	5×10^{26}	10^{-3}	700	45.0	5451	9500	0.55	–	4088	6900	–	0.02	0.01
#pmd3a2	5×10^{26}	10^{-3}	1000	45.0	3163	9500	0.23	–	2844	8000	–	0.01	0.01
#ocd1a2	5×10^{28}	10^{-2}	700	45.0	42 016	10 000	4.5	0.01	8979	2320	1850	0.03	0.02
#ocd2a2	5×10^{28}	10^{-2}	1000	45.0	34 922	10 000	3.7	0.01	7953	2456	2100	0.03	0.02
#ocd3a2	5×10^{28}	10^{-2}	3000	45.0	18 497	10 000	2.0	0.006	7056	3960	3800	0.02	0.01
#ocd1a3	5×10^{28}	10^{-2}	700	67.5	45 447	10 000	4.8	0.003	8449	2064	5800	0.015	0.005
#ocd2a3	5×10^{28}	10^{-2}	1000	67.5	37 811	10 000	4.0	0.003	8038	2343	7000	0.015	0.005
#ocd3a3	5×10^{28}	10^{-2}	3000	67.5	20 201	10 000	2.2	–	7373	3890	–	0.008	0.002
#pcd1a3	5×10^{28}	10^{-2}	700	67.5	27 495	10 000	2.9	0.01	7558	2975	1300	0.02	0.015
#pcd2a3	5×10^{28}	10^{-2}	1000	67.5	22 385	10 000	2.4	0.008	8085	3846	1550	0.016	0.013
#pcd3a3	5×10^{28}	10^{-2}	3000	67.5	10 960	10 000	1.2	0.005	6112	5670	3000	0.008	0.008

Notes. The output parameters are: the distance from the nucleus center L_∞ at which the terminal velocity v_∞ has been achieved, the corresponding flight time t_∞ and rotational frequency $\nu_\infty = \omega/(2\pi)$, the distance L_{90} at which 90% of the terminal velocity has been reached and its corresponding time t_{90}. t_{rs} is the time at which the grain has started to rotate. Δ_{max} and Δ_{min} are the maximum and minimum amplitudes of an oscillating grain. #omd and #ocd label oblate ellipsoidal shapes ($a/b = 0.5$); #pmd and #pcd label prolate shapes ($a/b = 2.0$).

Fulle*, Ivanovski* et al. 2015,
Special issue on Rosetta, A&A


Latitude: -8.20°
Longitude: 358.49° E
Distance S/C-surface: 2.69 km
expected size
from 2.7 km:
NAC_2016-09-02T19.57.44.449Z_ID10_1397549001_F22.IMG

→ ROSETTA'S GIADA INSTRUMENT IN NUMBERS

MISSION: To measure mass, momentum and velocity of dust grains ejected from comet

- **19 669** hours of science operations
- **22** cover moves to protect GIADA during delicate mission phases
- **6 650** dust particles detected:
  - Cross section measured for **4825**
  - Momentum, mass and speed measured for **1825**
  - Cross section, momentum, mass and speed measured for **307**

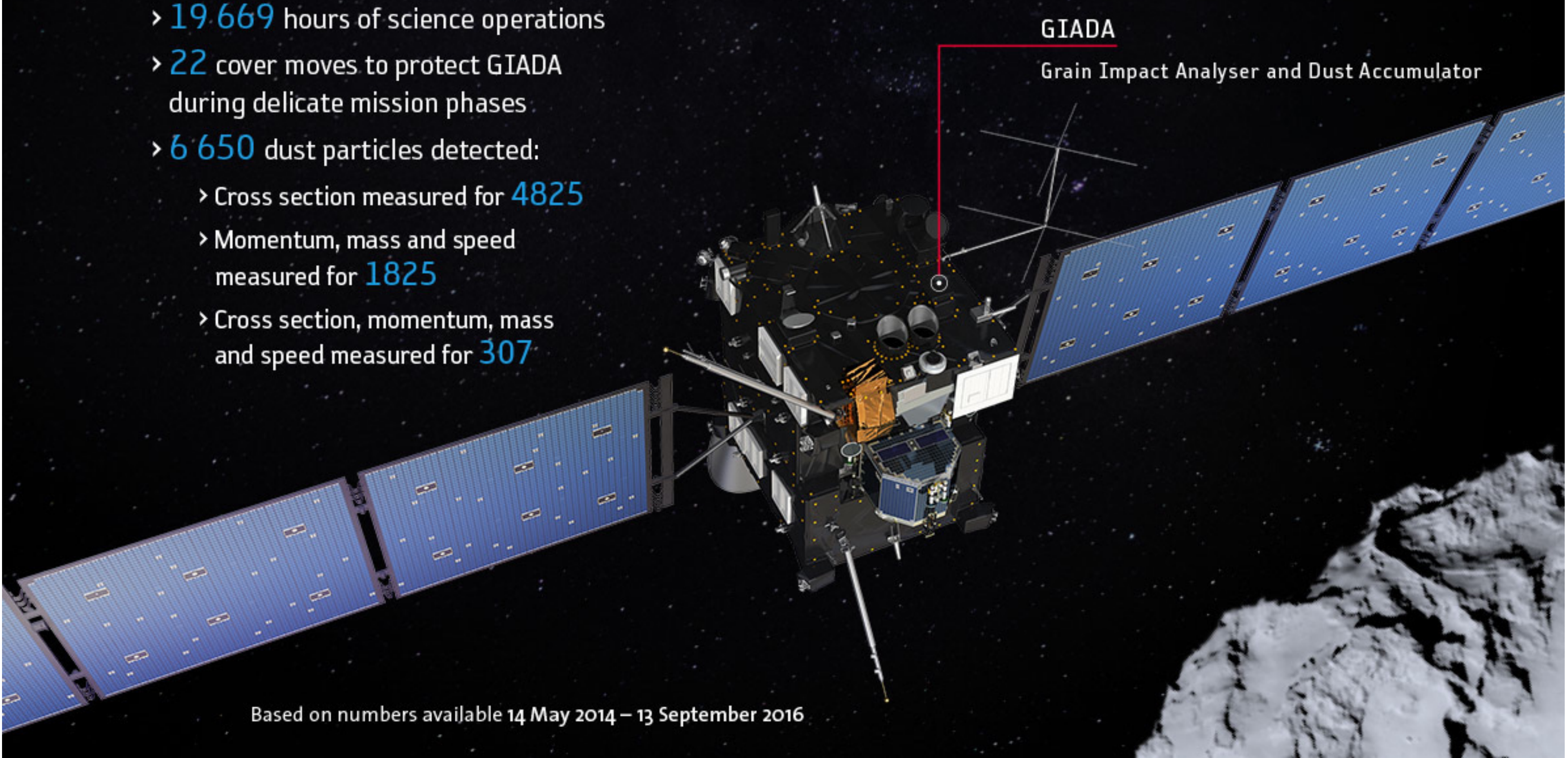

Based on numbers available 14 May 2014 – 13 September 2016

Are comets made of pebbles ?

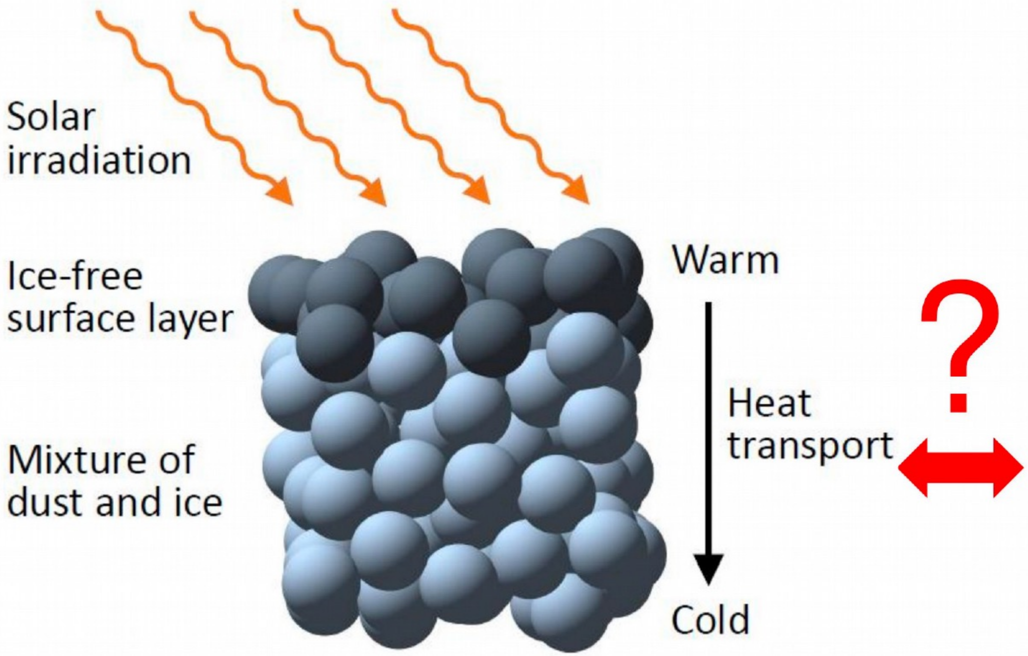

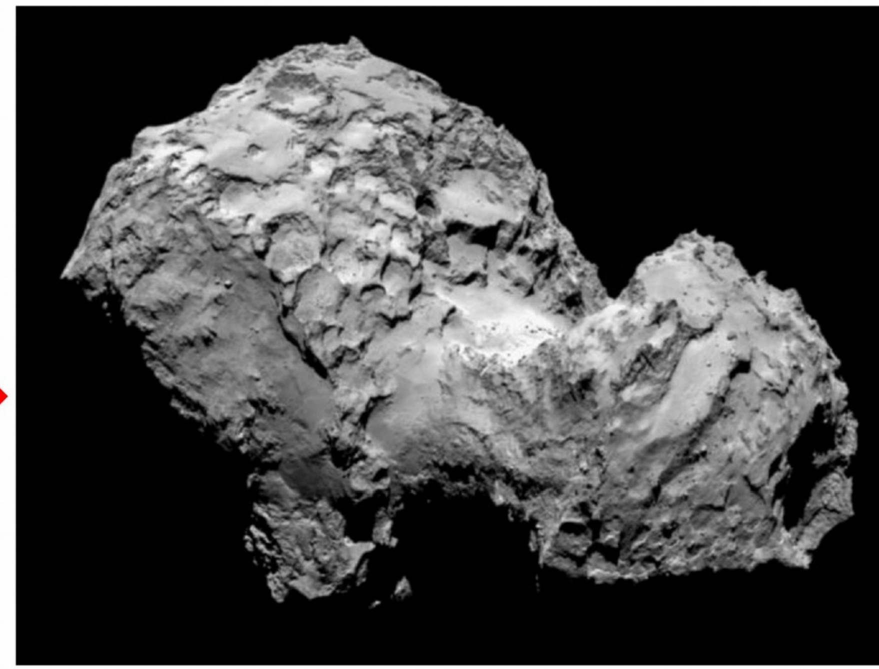

C/2020 F3 (NEOWISE)
11 – July -2020

Pebbles (if any) must be made of (icy) dust particles

Dust classification after IDPs, Rosetta, Stardust (Güttler et al 2019 AA 630, A24)

solid **group**

SOLID_1: ~100 nm

irregular grain

roundish monomer
(e.g., in computer models)

SOLID_2: dense aggregate of grains

< 1 mm

fluffy **group**

FLUFFY_1: fractal, dendritic agglomerate
(with $m \propto r^{D_f}$ and D_f typically 1.5 .. 2.5)

< 1 cm

porous **group**

POROUS_1: porous agglomerate

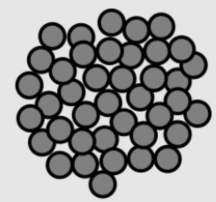

"average"
dust particle
< 1 cm

POROUS_2: cluster of agglomerates
(hierarchic)

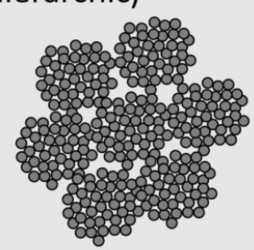

"pebble"
~1 cm

Physical evolution of comets

- If comets get close to the Sun and exhibit activity, comets have relatively short life times due to several effects:
  - Orbital instability
  - Loss of volatiles
  - Fragmentation
- Eventually, they may transform into inactive bodies of asteroidal type

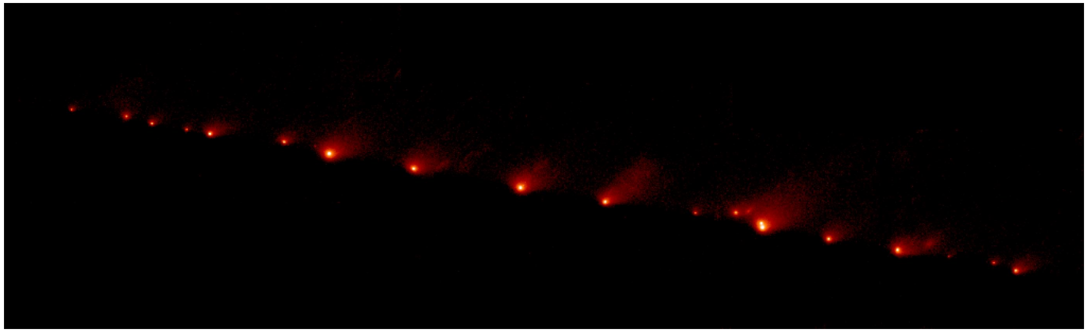

Fragmentation of comet Shoemaker-Levy 9 after a close approach with Jupiter

Comet composition

- Comets exhibit both volatile and refractory compounds
- Most volatiles are ices
  - Water ice is a main constituent that dominates the activity and the physical evolution of the comet
  - CO ice, more volatile than water ice, explains the cometary activity observed at large distances from the Sun
  - A large number of molecules have been found, especially organic ones, with abundances varying from comet to comet
- Most refractories are silicates
  - Non volatiles are studied through observations of the cometary dust
  - Dust observations: (1) astronomical observations in the infrared, (2) measurements *in situ* by space probes, (3) analysis of interplanetary dust particles collected on Earth

TABLE 2 **Measured and Observed Species in Comets**

Atoms + Molecules	Ions
H, C, O, S, Na, Fe, Ni, CO, CS, NH, OH, C_2, $^{12}C^{13}C$, CH, CN, ^{13}CN, S_2, SO, H_2, CO_2, HDO, CHO, HCN, DCN, $H^{13}CN$, OCS, SO_2, C_3, NH_2, H_2O, H_2S, HCO, H_2CS, C_2H_2, HNCO, H_2CO, CH_4, HC_3N, CH_3OH, CH_3CN, NH_2CHO, C_2H_6	C^+, N^+, O^+, Na^+, CO^+, CH^+, CN^+, OH^+, NH^+, H_2O^+, HCO^+, CO_2^+, C_3^+, CH_2^+, H_2S^+, NH_2^+, HCN^+, DCN^+, CH_3^+, H_3O^+, H_3S^+, NH_3^+, C_3H^+, CH_4^+, H_3CO^+, CH_5^+, $C_3H_3^+$

Organic molecules in 67/P

Results from the Rosina mass spectrometer on board of the *Rosetta* mission

Brown: new detections

Interplanetary dust

- Zodiacal light
  - Zodiacal light is due to sunlight scattered by a broad interplanetary dust cloud aligned with the ecliptic plane
  - Zodiacal light brightness is a function of viewing direction, wavelength, heliocentric distance and position of the observer relative to the dust symmetry plane
- Infrared zodiacal emission
  - At $\lambda \gtrsim 3$ μm, thermal emission from the interplanetary dust (zodiacal emission) dominates over scattered light
  - The emission varies along the ecliptic plane and is a critical disturbing factor in extragalactic infrared astronomy

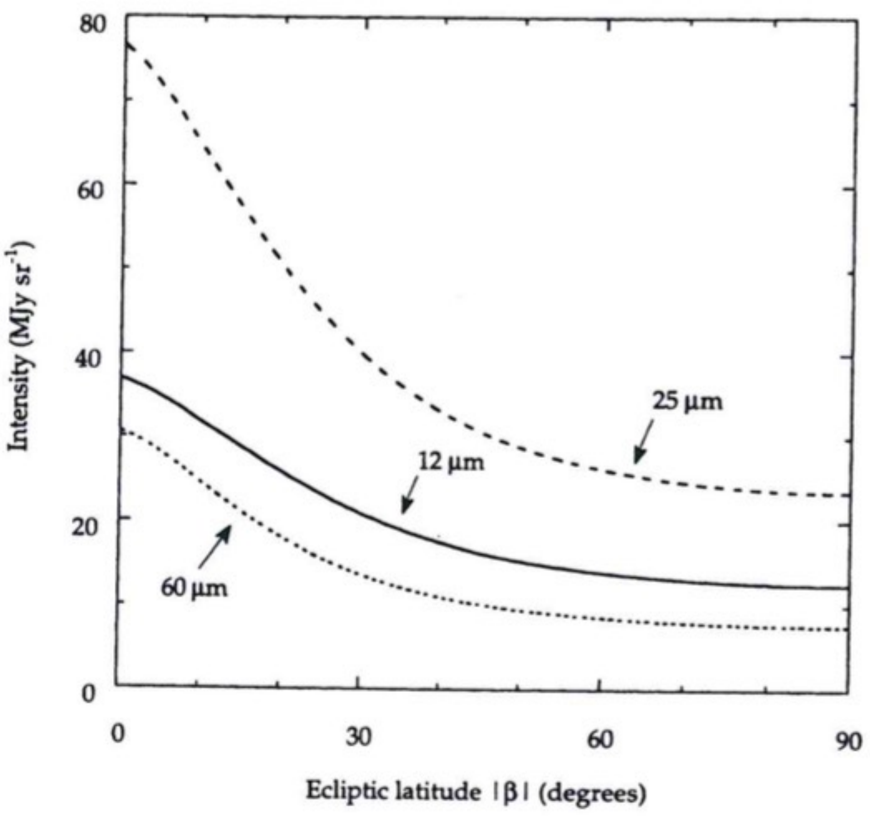

Interplanetary dust

Interplanetary dust particles collected in the stratosphere by NASA's cosmic dust program

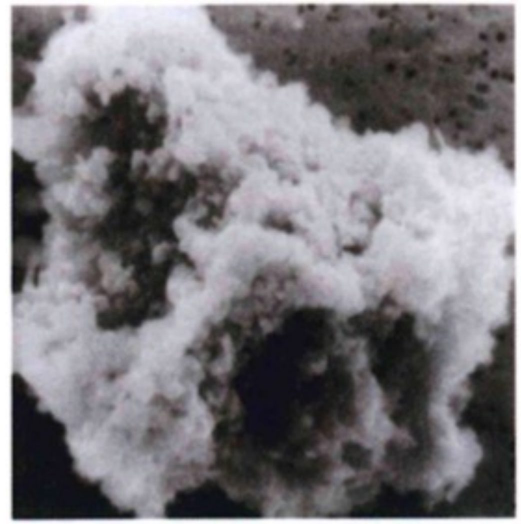

Top:
grain of chondritic composition

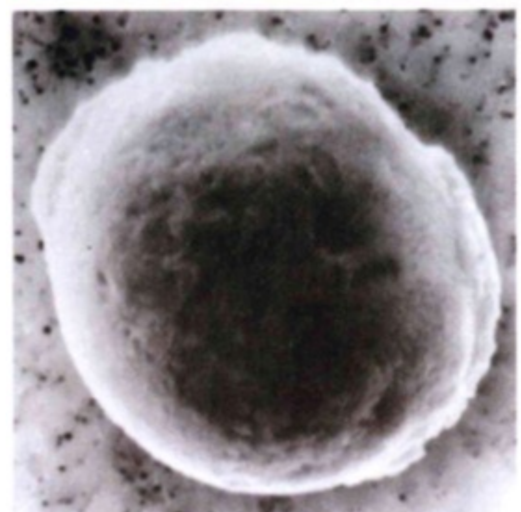

Bottom:
Fe-S-Ni sphere

Image sizes:
30 μm

Virtual Observatory data service of NASA DUST CATALOG with spectra and images will be maintained from 2021 by Osservatorio Astronomico di Trieste